Enhancing Low-Field MRI (LF-MRI) for Non-Invasive Brain Stimulation (NIBS) Applications

Hengameh Marzbani[1,2], Elizabet Gregory[1,3], Annika MacKenzie[1,4], Sharada Balaji[4], Shannon Kolind[4,5,6,7]
Fidel Vila-Rodriguez[1,2,3,7]

[1]Non-Invasive Neurostimulation Therapies (NINET) Laboratory, [2]School of Biomedical Engineering, Faculty of Applied Science | Faculty of Medicine, [3]Department of Psychiatry, Faculty of Medicine, [4]Department of Physics and Astronomy, [5]Division of Neurology, Department of Medicine, [6]Department of Radiology, [7]Djavad Mowafaghian Centre for Brain Health, University of British Columbia

Introduction

Access to High-field MRI (HF_{MRI}) scanners is limited by geographic disparities, high per-patient expenses, and the exclusion of individuals ineligible for traditional MRIs. This highlights the need for low-field MRI (LF_{MRI}) scanners[1]. However, the typically lower resolution of LF_{MRI} necessitates the use of enhancement techniques to improve image quality for personalized non-invasive brain stimulation (NIBS). In this study, we aim to evaluate the effectiveness of these enhanced images for NIBS applications.

Methods

Twenty individuals underwent HF_{MRI} (3T) and LF_{MRI} (0.064T) structural imaging. Following data quality assessment and pre-processing, the SynthSR super-resolution method generated synthesized LF_{MRI} scans[2]. Electric field (e-field) modeling was performed for LF_{MRI}, SynthSR-LF_{MRI} variants, and HF_{MRI} using SimNIBS, enabling tissue segmentation and conversion into tetrahedral mesh head models[3,4]. Then, we calculated Dice coefficients of voxel overlap with the $HF_{MRI.}$

Results

CHARM segmentation

Comparison of tissue segmentation and Dice coefficients of LF variants with the HF_{MRI} for grey matter, white matter, and CSF are shown Figure 1. The repeated measures ANOVA revealed that SynthSR-LF_{MRI} and PseudoT1Synthsr-LF_{MRI} outperformed LF_{MRI} (p<0.001), while SynthSR-LF_{MRI} and PseudoT1Synthsr-LF_{MRI} performed similarly across white matter, grey matter, and CSF (p=0.17-1.00). Table 1 shows the comparison of average dice coefficients for tissue segmentation and E-field modeling across HF_{MRI} and LF_{MRI} variants.

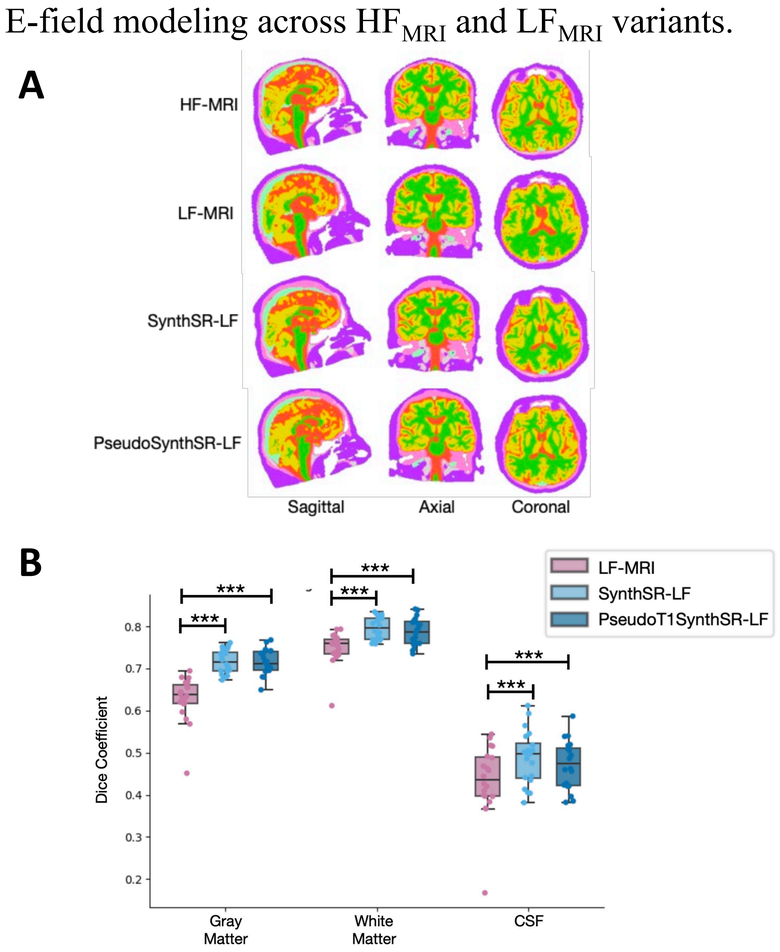

Figure 1. A) CHARM tissue segmentations. **B)** Similarity of CHARM segmentation to the HF scan, as measured by Dice coefficients.

Table 1. Comparison of average dice coefficients for tissue segmentation and E-field modeling across HF_{MRI} and LF_{MRI} variants.

	White Matter	Grey Matter	CSF	99.9 percentile	99 percentile	75 percentile
	Mean (SD)					
HF vs. SynthSR-LF	0.80 (0.03)	0.72 (0.03)	0.49 (0.06)	0.32 (0.16)	0.59 (0.08)	0.65 (0.03)
HF vs. PseudoT1Synthsr-LF	0.79 (0.03)	0.71 (0.03)	0.47 (0.06)	0.33 (0.15)	0.54 (0.10)	0.62 (0.04)
HF vs. LF	0.75 (0.04)	0.63 (0.05)	0.43 (0.08)	0.28 (0.16)	0.48 (0.16)	0.52 (0.09)

Electrical field modeling

We assessed the correspondence of e-field modeling through measures of both magnitude and Dice scores for the spatial distribution of e-fields within the left dorsolateral prefrontal cortex (DLPFC) target. Qualitative and quantitative differences between the e-field distribution and magnitude between HF_{MRI} and LF variants are shown at the group-level. Results demonstrate e-field magnitude values in the 10mm ROI surrounding the target were on average slightly overestimated by all LF variants.

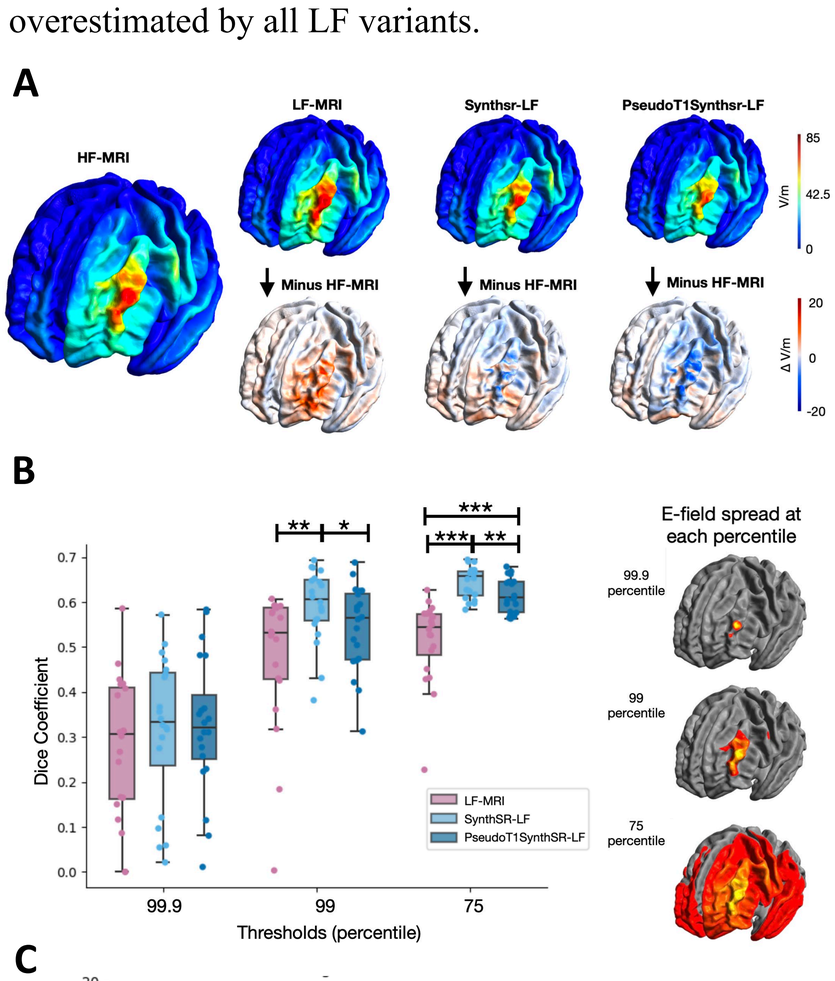

Figure 2. A) E-field simulations. Contrasts of each LF variant (minus HF_{MRI}) demonstrate the spatial distribution of bias. **B)** Bias of the e-field magnitude for each LF variant. **C)** Quantification of similarity of e-field spread, as measured by the Dice coefficient across varying percentile.

Also, repeated measures ANOVA showed significantly higher Dice coefficients for voxel overlap in e-field distribution at 99th and 75th percentiles for SynthSR-LF_{MRI} variants compared to the HF_{MRI} (Bonferroni-corrected p <0.01), whereas no significant result was observed between LF_{MRI} and HF_{MRI}.

Application in Neuronavigation

To assess the LF_{MRI} utility for precision NIBS delivery, we conducted neuronavigation in two healthy subjects, using Localite TMS Navigator. For each session, one of each of the MRI scans (HF_{MRI}, LF_{MRI}, SynthSR-LF_{MRI} and PseudoT1SynthSR-LF_{MRI}) was loaded in. Target and entry locations were calculated with LDLPFC target. Among all SynthSR-LF_{MRI} variants, PseudoT1SynthSR-LF_{MRI} achieved the most accurate target localization, with results closest to the HF_{MRI} target coordinate (within 5 mm).

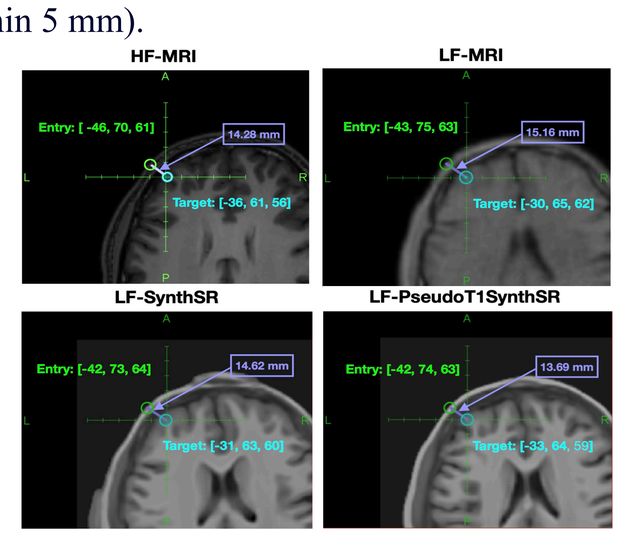

Figure 3. Neuronavigation was performed using the HF_{MRI}, and each of the LF variants, with targets positioned at the [-38, 44, 26] MNI coordinates, and entry points calculated following subject registration. Distances between target and entry pairs presented were computed. All coordinates presented for the LF variants are in the HF_{MRI} space.

Conclusion

Our results show that the SynthSR method can enhance the reliability of LF_{MRI} scans in segmentation accuracy and e-field modeling, achieving performance levels comparable to HF_{MRI} scans. Additionally, our data suggest that LF_{MRI} may be a feasible input for target localization in neuronavigation systems.

Clarifying Terminology

In this work, we refer to raw acquisitions as HF_{MRI} (3T) and LF_{MRI} (0.064T), while SynthSR-LF_{MRI} and PseudoT1SynthSR-LF_{MRI} denote post-processed low-field MRI scans using the SynthSR super-resolution method, with T1-weighted and T2-weighted LF_{MRI} inputs, respectively.

References

1. Kimberly, W. Taylor, et al. "Brain imaging with portable low-field MRI." Nature Reviews Bioengineering 1.9 (2023): 617-630.
2. Iglesias, Juan Eugenio, et al. "Joint super-resolution and synthesis of 1 mm isotropic MP-RAGE volumes from clinical MRI exams with scans of different orientation, resolution and contrast." Neuroimage 237 (2021): 118206.
3. Thielscher A, Antunes A, Saturnino GB. Field modeling for transcranial magnetic stimulation: A useful tool to understand the physiological effects of TMS? Annu Int Conf IEEE Eng Med Biol Soc 2015;2015:222–5.https://doi.org/10.1109/EMBC.2015.7318340.
4. Puonti O, Van Leemput K, Saturnino GB, Siebner HR, Madsen KH, Thielscher A. Accurate and robust whole-head segmentation from magnetic resonance images for individualized head modeling. NeuroImage 2020;219:117044.

Acknowledgement

We are grateful to the study participants for their enrollment. Also, we acknowledge the Dr. Djavad Mowafaghian Centre for Brain Health (DMCBH) for providing us with services to acquire the dataset.

THE UNIVERSITY OF BRITISH COLUMBIA

NINET non invasive neurostimulation therapies

SBME UBC SCHOOL OF BIOMEDICAL ENGINEERING Faculties of Applied Science and Medicine